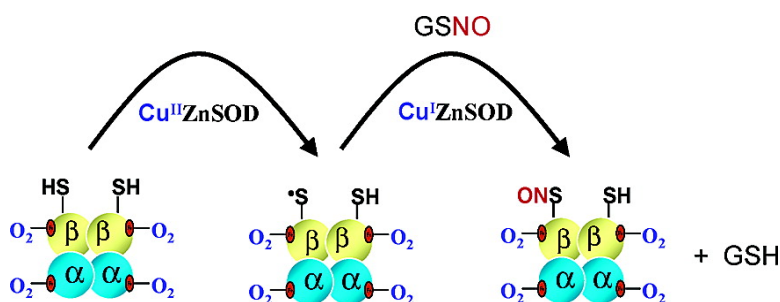


## Superoxide Dismutase Targets NO from GSNO to Cys $\beta$ 93 of Oxyhemoglobin in Concentrated but Not Dilute Solutions of the Protein

Andrea A. Romeo, John A. Capobianco, and Ann M. English

*J. Am. Chem. Soc.*, **2003**, 125 (47), 14370-14378 • DOI: 10.1021/ja0289752 • Publication Date (Web): 31 October 2003

Downloaded from <http://pubs.acs.org> on March 30, 2009



### More About This Article

Additional resources and features associated with this article are available within the HTML version:

- Supporting Information
- Access to high resolution figures
- Links to articles and content related to this article
- Copyright permission to reproduce figures and/or text from this article

[View the Full Text HTML](#)

## Superoxide Dismutase Targets NO from GSNO to Cys $\beta$ 93 of Oxyhemoglobin in Concentrated but Not Dilute Solutions of the Protein

Andrea A. Romeo, John A. Capobianco, and Ann M. English\*

Contribution from the Department of Chemistry and Biochemistry, Concordia University,  
1455 de Maisonneuve Boulevard West, Montreal, Quebec Canada H3G 1M8

Received October 16, 2002; E-mail: english@vax2.concordia.ca

**Abstract:** The role of hemoglobin (Hb) in transmitting the vasodilatory property of NO throughout the vascular system is of much current interest. NO exchange between Hb and low-molecular-weight nitrosothiols such as S-nitrosoglutathione (GSNO) has been speculated and reported in vitro. Previously, we reported that NO delivery from GSNO to Cys $\beta$ 93 of human oxyHb is prevented in the presence of the Cu chelators, neocuproine, and DTPA.<sup>1</sup> In the present work, 5 mM solutions of commercial human Hb were found by ICP-MS to contain  $\sim 20 \mu\text{M}$  Cu and Zn, suggesting the presence of Cu,Zn-superoxide dismutase (CuZnSOD), which was confirmed by Western blotting. SOD activity measurements were consistent with the presence of  $\sim 20 \mu\text{M}$  CuZnSOD monomer in 5 mM Hb solutions, which is the physiological concentrations of these proteins in the red blood cell. Incubation of 3.75 mM oxyHb (15 mM heme; 7.5 mM Cys $\beta$ 93) with 3.75 or 7.5 mM GSNO gave rise to 50% or 100% S-nitrosation, respectively, of Cys $\beta$ 93 as monitored by FTIR  $\nu(\text{SH})$  absorption, whereas excess GSNO over Cys $\beta$ 93 converted oxyHb to metHb due to the reaction, oxyHb + NO  $\rightleftharpoons$  metHb + NO<sub>3</sub><sup>-</sup>. Removal of CuZnSOD by anion-exchange chromatography yielded an oxyHb sample that was *unreactive* toward GSNO, and replacement with bovine CuZnSOD restored reactivity. Addition of 1  $\mu\text{M}$  GSNO (Cys $\beta$ 93/GSNO = 1) to solutions diluted 10<sup>4</sup>-fold from physiological concentrations of oxyHb and CuZnSOD resulted largely in metHb formation. Thus, this work reports the following key findings: CuZnSOD is an efficient catalyst of NO transfer between GSNO and Cys $\beta$ 93 of oxyHb; metHb is not detected in oxyHb/GSNO incubates containing close to the physiological concentration (5 mM) of Hb and CuZnSOD when the Cys $\beta$ 93/GSNO molar ratio is 0.5 to 1.0, but metHb is detected when the total Hb concentration is low micromolar. These results suggest that erythrocyte CuZnSOD may play a critical role in preserving the biological activity of NO by targeting it from GSNO to Cys $\beta$ 93 of oxyHb rather than to its oxyheme.

### Introduction

The interaction between nitric oxide (NO) and the conserved Cys $\beta$ 93 of hemoglobin (Hb) in red blood cells (RBCs) has been of intense interest recently.<sup>2–5</sup> The allosteric transition of Hb reportedly controls the affinity of Cys $\beta$ 93 for NO, providing a mechanism for NO capture and delivery that is sensitive to the partial pressure of oxygen. Such a mechanism would allow matching of blood flow and tissue oxygenation. GSNO, the S-nitroso form of the dominant low-molecular weight thiol in RBCs,<sup>6</sup> and CysNO are possible NO donors to Cys $\beta$ 93 of oxyhemoglobin (oxyHb; HbFe<sup>II</sup>O<sub>2</sub>) which has a higher affinity for NO than its deoxy form (deoxyHb; HbFe<sup>II</sup>).<sup>7</sup>

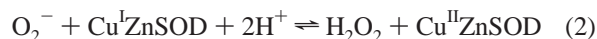
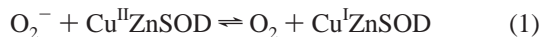
A direct *trans*-S-nitrosation reaction (i.e., NO<sup>+</sup> transfer) has been proposed.<sup>8</sup> However, unlike direct *trans*-S-nitrosation that is reportedly not metal-catalyzed,<sup>9</sup> we have shown that S-nitrosation of oxyHb at Cys $\beta$ 93 requires the presence of copper<sup>1</sup> as was also reported for Cys34 of bovine serum albumin (BSA).<sup>10</sup> Furthermore, we have demonstrated<sup>11,12</sup> that neocuproine, a Cu<sup>I</sup>-specific chelator [ $E^\circ(\text{Cu}^{\text{II/I}}) = 0.58 \text{ V}$ ],<sup>12</sup> inhibits NO release from GSNO in solutions of oxyHb or deoxyHb. These observations are consistent with the extensive literature revealing that trace Cu<sup>I</sup> serves as a highly efficient catalyst of RSNO breakdown.<sup>9</sup>

CuZnSOD, a homodimer containing one Cu and one Zn atom per monomer, is the major source of copper in RBCs. Present

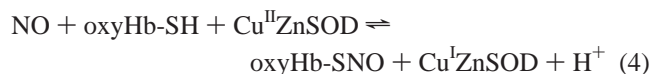
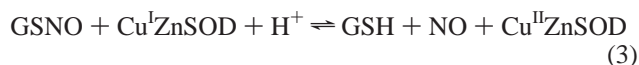
- (1) Romeo, A. A.; Filosa, A.; Capobianco, J. A.; English, A. M. *J. Am. Chem. Soc.* **2001**, *123*, 1782–1783.
- (2) Lane, P.; Gross, S. *Nat. Med.* **2002**, *8*, 657–658.
- (3) McMahon, T. J.; Moon, R. E.; Lusching, B. P.; Carraway, M. S.; Stone, A. E.; Stolp, B. W.; Gow, A. J.; Pawloski, J. R.; Watke, P.; Singel, D. J.; Piantadosi, C. A.; Stamler, J. S. *Nat. Med.* **2002**, *8*, 711–717.
- (4) Gross, S. S.; Lane, P. *Proc. Natl. Acad. Sci. U.S.A.* **1999**, *96*, 9967–9969.
- (5) Patel, R. P.; Hogg, N.; Spencer, N. Y.; Kalyanaraman, B.; Matalon, S.; Darley-Usmar, V. M. *J. Biol. Chem.* **1999**, *274*, 15487–15492.
- (6) Singh, S. P.; Wishnok, J. S.; Keshive, M.; Deen, W. M.; Tannenbaum, S. R. *Proc. Natl. Acad. Sci. U.S.A.* **1996**, *93*, 14428–14433.

- (7) Stamler, J. S.; Jia, L.; Eu, J. P.; McMahon, T. J.; Demchenko, I. T.; Bonaventura, J.; Gernert, K.; Piantadosi, C. A. *Science* **1997**, *276*, 2034–2037.
- (8) Jia, L.; Bonaventura, C.; Bonaventura, J.; Stamler, J. S. *Nature* **1996**, *380*, 221–226.
- (9) Williams, D. L. H. *Acc. Chem. Res.* **1999**, *32*, 869–876.
- (10) Tsikas, D.; Sandmann, J.; Luessen, P.; Savva, A.; Rossa, S.; Stichtenoth, D. O.; Frolich, J. C. *Biochim. Biophys. Acta* **2001**, *1546*, 422–434.
- (11) Romeo, A. A.; Capobianco, J. A.; English, A., M. *J. Biol. Chem.* **2002**, *277*, 24135–24141.
- (12) Lei, Y.; Anson, F. C. *Inorg. Chem.* **1995**, *34*, 1083–1089.

at a concentration of  $\sim 20 \mu\text{M}$  monomer,<sup>13</sup> the assumed function of erythrocyte CuZnSOD is to eliminate  $\text{O}_2^-$  released from oxyHb.<sup>14</sup> The catalytic cycle of CuZnSOD involves redox turnover of copper:<sup>15</sup>



We demonstrate here that redox turnover of erythrocyte CuZnSOD also allows it to function *in vitro* as an NO S-transferase, catalyzing NO transfer from GSNO to Cys $\beta$ 93 of oxyHb:



Results are presented that may support a role for CuZnSOD in catalyzing the reductive cleavage of GSNO (or other RSNOs in the RBC), and in targeting the NO released to Cys $\beta$ 93 of oxyHb. Our experiments were carried out using GSNO concentrations  $> 10^6$ -fold higher than those expected *in vivo*, which gives rise to stable S-nitrosated Hb (Hb-SNO) in contrast to the instability of Hb-SNO when overproduced in RBCs.<sup>16</sup> Nonetheless, CuZnSOD-catalyzed S-nitrosation, observed at *physiological* concentrations of oxyHb, may explain in part why RBCs do not convert all the endogenous NO produced in the vascular system to  $\text{NO}_3^-$  as anticipated from the efficiency of NO trapping experiments (reaction 5) carried out using non-physiological (micromolar) concentrations of oxyHb.<sup>17</sup>



Formation of  $\text{NO}_3^-$  would result in loss of NO bioactivity and as shown here, CuZnSOD may play a critical role in preventing this. Significantly, copper added as  $\text{CuSO}_4$  does not exhibit the same NO-targeting ability as CuZnSOD.

The reported absence of arterial-venous gradients of Hb-SNO in humans<sup>18</sup> and their presence in rats<sup>8,19</sup> provides contradictory evidence that delivery of  $\text{O}_2$  and NO to tissues are allosterically coupled events. However, such gradients are questionable given the widely varying reports of Hb-SNO levels ( $< 20 \text{ nM}$  to  $5 \mu\text{M}$ ) in arterial and venous blood.<sup>8,18,20–22</sup> Furthermore, although kinetic and thermodynamic arguments have been made to support the  $\text{O}_2$ -linked, allosterically mediated release of NO from Hb-SNO,<sup>8,19,23</sup> the physiological relevance of such linkage has

been challenged on the basis of the very high  $\text{O}_2$  affinity of Hb-SNO, which could potentially limit its role in the control of NO delivery.<sup>3,5,24–26</sup> A detailed understanding of the mechanism of Hb S-nitrosation and denitrosation in RBCs is clearly critical in delineating the role of Hb in NO transport. The present study is an important first step in this direction, since evidence is provided for a possible mechanism involving CuZnSOD-catalyzed S-nitrosation of Cys $\beta$ 93 of oxyHb.

## Experimental Procedures

**Materials.** Human hemoglobin A (Sigma) and bovine erythrocyte CuZnSOD (Roche Molecular Biochemicals) were used without further purification except where indicated. A rabbit polyclonal antibody developed against human CuZnSOD (0.85 mg/mL SOD-100) and a goat anti-rabbit HRP-conjugated antibody (SAB-301) were purchased from Stressgen Biotechnologies. All reagents were of the highest quality available and were obtained from the following suppliers: GSNO [glycine, *N*-(*N*-L- $\gamma$ -glutamyl-S-nitroso-L-cysteinyl)] and DEA/NO [diethylammonium (*Z*)-1-(*N,N*-diethylamino)diazen-1-ium-1,2-diolate], Caymen;  $\text{Na}_2\text{EDTA}$  (ethylenediamine-*N,N,N',N'*-tetraacetic acid, disodium salt), neocuproine (2,9-dimethyl-1,10-phenanthroline), GSH, GSSG, and DEAE-Sephacel anion exchanger, Sigma; trace-metal grade HCl, pyrogallol (1,2,3-trihydroxybenzene), sodium dithionite, and sodium phosphate salts, Fisher; DTPA (diethylenetriamine-*N,N,N',N',N''*-pentaacetic acid) and Tris *Ultrapure*, ICN; cacodylic acid (dimethyl-arsenic acid), Aldrich; CuCl and  $\text{CuSO}_4 \cdot 5\text{H}_2\text{O}$ , Anachemia; isoamyl alcohol, Baker; *OmniTrace* Ultrahigh Purity concentrated  $\text{HNO}_3$ , EM Science; 30%  $\text{H}_2\text{O}_2$ , 1000 ppm Cu, Fe, Mn, and Zn standard solutions, ACP Chemicals Inc., Montreal; NAP-5 ( $0.9 \times 2.8 \text{ cm}^2$ ) and HiTrap 5-mL ( $1.6 \times 2.5 \text{ cm}$ ) Sephadex G-25 columns, Amersham Pharmacia Biotech. Nanopure water (specific resistance  $18 \text{ M}\Omega\text{-cm}$ ), obtained from a Millipore Simplicity water purification system and treated with Chelex-100 (Sigma) to remove trace metal ions, was used to prepare all buffers and  $\text{H}_2\text{O}$  solutions.

**Methods.** Stock solutions of 250 mM GSNO in 200 mM sodium phosphate buffer, pH 7.2 (NaPi) were prepared  $< 2$  min before use in a glovebox (MBraun, Model MB-OX-SE1). The final pH was adjusted to pH 7.2, and the GSNO concentration was determined spectrophotometrically ( $\epsilon_{333,5\text{nm}} = 774 \text{ M}^{-1} \text{ cm}^{-1}$ ).<sup>27</sup> Stock DEA/NO was prepared in 0.01 M NaOH at  $0^\circ\text{C}$  and added to NaPi in the glovebox immediately before use. The DEA/NO concentration was determined using  $\epsilon_{520\text{nm}} = 6500 \text{ M}^{-1} \text{ cm}^{-1}$ . Stock solutions of DTPA (15 mM) and neocuproine (650  $\mu\text{M}$ ) were also prepared in NaPi.

**Preparation and UV-vis Analysis of the Hb Incubates.** The Hb samples were prepared as described previously.<sup>11</sup> Briefly, lyophilized metHb from the bottle was dissolved in NaPi and centrifuged at 12 000 rpm for 2 min, and the supernatant was stored at  $4^\circ\text{C}$  prior to use. The metHb (HbFe<sup>III</sup>) concentration was determined spectrophotometrically ( $\epsilon_{500\text{nm}} = 10 \text{ mM}^{-1} \text{ cm}^{-1}$  per heme and  $\epsilon_{630 \text{ nm}} = 4.4 \text{ mM}^{-1} \text{ cm}^{-1}$  per heme)<sup>28,29</sup> in an FTIR-type cell with a 6- $\mu\text{m}$  Teflon spacer (Harrick) using a custom-made bracket in a Beckman DU 650 UV-vis spectrophotometer. Samples of oxyHb were prepared in the glovebox by treating metHb with a slight excess of sodium dithionite, desalting on the HiTrap column, and introducing a small volume of air into the sample by syringe.<sup>30</sup> The deoxyHb concentrations were determined

- (13) Gartner, A.; Weser, U. *FEBS Lett.* **1983**, *155*, 15–18.  
 (14) Dershwitz, M.; Novak, R. F. *J. Biol. Chem.* **1982**, *257*, 75–79.  
 (15) Forman, H. J.; Evans, H. J.; Hill, R. L.; Fridovich, I. *Biochemistry* **1973**, *12*, 823–827.  
 (16) Gladwin, M. T.; Wang, X.; Reiter, C. D.; Yang, B. K.; Vivas, E. X.; Bonaventura, C.; Schechter, A. N. *J. Biol. Chem.* **2002**, *277*, 27818–27828.  
 (17) Doyle, M. P.; Hoekstra, J. W. *J. Inorg. Biochem.* **1981**, *14*, 351–358.  
 (18) Gladwin, M. T.; Ognibene, F. P.; Pannell, L. K.; Nichols, J. S.; Pease-Fye, M. E.; Shelhamer, J. H.; Schechter, A. N. *Proc. Natl. Acad. Sci. U.S.A.* **2000**, *97*, 9943–9948.  
 (19) Gow, A. J.; Stamler, J. S. *Nature* **1998**, *391*, 169–173.  
 (20) Funai, E. F.; Davidson, A.; Seligman, S. P.; Finlay, T. H. *Biochem. Biophys. Res. Commun.* **1997**, *239*, 875–877.  
 (21) Jour'd'heuil, D.; Hallen, K.; Feelisch, M.; Grisham, M. B. *Free Radical Biol. Med.* **2000**, *28*, 409–417.  
 (22) Gladwin, M. T.; Shelhamer, J. H.; Schechter, A. N.; Pease-Fye, M. E.; Waclawiw, M. A.; Panza, J. A.; Ognibene, F. P.; Cannon, R. O., III. *Proc. Natl. Acad. Sci. U.S.A.* **2000**, *97*, 11482–11487.  
 (23) McMahon, T. J.; Exton Stone, A.; Bonaventura, J.; Singel, D. J.; Solomon Stamler, J. *J. Biol. Chem.* **2000**, *275*, 16738–16745.

- (24) Bonaventura, C.; Ferruzzi, G.; Tesh, S.; Stevens, R. D. *J. Biol. Chem.* **1999**, *274*, 24742–24748.  
 (25) Wolzt, M.; MacAllister, R. J.; Davis, D.; Feelisch, M.; Moncada, S.; Vallance, P.; Hobbs, A. J. *J. Biol. Chem.* **1999**, *274*, 28983–28990.  
 (26) Deem, S.; Gladwin, M. T.; Berg, J. T.; Kerr, M. E.; Swenson, E. R. *Am. J. Respir. Crit. Care Med.* **2001**, *163*, 1164–1170.  
 (27) Scorza, G.; Pietraforte, D.; Minetti, M. *Free Radical Biol. Med.* **1997**, *22*, 633–642.  
 (28) Antonini, E.; Wyman, J.; Brunori, M.; Taylor, F. J.; Rossi Farinelli, A.; Caputo, A. *J. Biol. Chem.* **1964**, *239*, 907–912.  
 (29) Van Assendelft, O. W.; Zijlstra, W. G. *Anal. Biochem.* **1975**, *69*, 43–48.

using  $\epsilon_{555\text{ nm}} = 12.5\text{ mM}^{-1}\text{ cm}^{-1}$  per heme, and oxyHb concentrations using  $\epsilon_{541\text{ nm}} = 13.5\text{ mM}^{-1}\text{ cm}^{-1}$  per heme and  $\epsilon_{576\text{ nm}} = 14.6\text{ mM}^{-1}\text{ cm}^{-1}$  per heme.<sup>30</sup> Use of the FTIR-type cell with a 6- $\mu\text{m}$  path length to record the optical spectra of the products formed in the Hb/GSNO incubates allowed measurements to be made close to the physiological concentration of Hb ( $\sim 5\text{ mM}$ ).<sup>31</sup>

Optical spectra were recorded using a scan time of 1200 nm/min and analyzed<sup>11</sup> using multicomponent-analysis software (Beckman, PN 517031) for the DU 600 spectrophotometer. The software uses Full Spectrum Quantitation (FSQ) to calculate the concentration of each component in a mixture by performing a Fourier transform on the scan data. Each point in the calculated absorbance transform contains information from all of the data points in the absorbance scan. The absorbance transform follows Beer's law.

**FTIR Spectra of the Hb Incubates.** To record the Fourier transform infrared (FTIR) spectra in the SH stretching  $\nu(\text{SH})$  region ( $\sim 2500\text{ cm}^{-1}$ ), 20  $\mu\text{L}$  of 7 mM Hb (28 mM heme) in NaPi was added by syringe onto a 13-mm  $\text{CaF}_2$  window and the FTIR cell was immediately assembled with a 250- $\mu\text{m}$  Teflon spacer (Harrick). Spectra were recorded at 25 °C on a Nicolet Magna-IR 550 spectrometer with a MCT detector cooled to 77 K and purged with dry air from a Whatman FTIR Purge (model 75-52). All reported spectra are an average of 500 scans recorded in 5.5 min at a resolution of 2  $\text{cm}^{-1}$  using a Happ-Genzel apodization with a velocity and aperture of 4.4303 cm/s and 2, respectively. Omnic (Nicolet) software was used for spectral analysis as previously reported.<sup>11</sup>

**ESI-MS Analysis.** Hb solutions (7.0 mM) in NaPi were diluted 10<sup>3</sup>-fold with H<sub>2</sub>O to give  $\sim 0.5\text{ }\mu\text{g}/\mu\text{L}$  protein. Aliquots were infused into the ESI source of the mass spectrometer (ThermoFinnigan SSQ 7000) by flow injection from the HPLC (Agilent 1090) using a 100- $\mu\text{L}$  loop (but no column) at 50  $\mu\text{L}/\text{min}$  with 75%  $\text{CH}_3\text{CN}/0.05\%$  TFA as a mobile phase. The 250 mM GSH, GSNO, and GSSG stocks in NaPi were diluted 500-fold with H<sub>2</sub>O and then 10-fold to 50  $\mu\text{M}$  with 75%  $\text{CH}_3\text{CN}/0.05\%$  TFA, and their mass spectra were obtained as for the Hb solutions.

**ICP-MS Analysis.** A PE Sciex Elan 6000 inductively coupled plasma mass spectrometer (ICP-MS) with a cross-flow nebulizer and Scott-type spray chamber was used to determine the amount of Cu, Zn, and Fe in the samples and buffers as described previously.<sup>11</sup> Stock Hb solutions in NaPi were added to 50  $\mu\text{L}$  of 30% H<sub>2</sub>O<sub>2</sub> and 500  $\mu\text{L}$  of ultrahigh purity concentrated HNO<sub>3</sub> to give a final heme iron concentration of  $\sim 5\text{ mM}$ , and the samples were ashed using a Bunsen burner. The residue was dissolved in 10 mL of 5% (v/v) HNO<sub>3</sub>, and ICP-MS analyses for Cu, Fe, and Zn were performed. An internal standard of 9 nM (0.500 ppb) Mn prepared from a 1000 ppm Mn standard solution was added to all samples. Standard analyte curves were prepared by diluting 1000 ppm Cu, Zn, and Fe standards in 5% (v/v) HNO<sub>3</sub> and Nanopure water to give 0–8  $\mu\text{M}$  (0–0.500 ppm) Cu and Zn and 0–9  $\mu\text{M}$  (0–0.500 ppm) Fe. The reported Cu and Zn concentrations are normalized to 20 mM Fe (5.0 mM Hb), and all values are the results of at least triplicate experiments with standard deviations of  $< 5\%$ .

**Dialysis and DEAE Purification of Hb Samples.** A solution of metHb from the bottle was extensively dialyzed at 4 °C versus Na<sub>2</sub>-EDTA (pH 7.0) followed by H<sub>2</sub>O, lyophilized, and dissolved in NaPi to a concentration of 30 mM heme as described previously.<sup>11</sup> For anion-exchange purification, metHb from the bottle was dissolved in 0.5 mL of NaPi to a concentration of 32 mM heme and added to a 0.9 cm  $\times$  2.8 cm DEAE-Sephacel anion-exchange column equilibrated with NaPi. The eluent was 100 mM NaCl in the same buffer, and the Hb that eluted between 1 and 2 mL was twice reapplied to the column to remove

**Table 1.** Determination of Cu and Zn in Stock Solutions by ICP-MS

sample <sup>a</sup>	Cu ( $\mu\text{M}$ )	Cu (ppm)	Zn ( $\mu\text{M}$ )	Zn (ppm)
5 mM Hb <sup>b</sup>	19 $\pm$ 3	1.207 $\pm$ 0.190	20 $\pm$ 2	1.307 $\pm$ 0.130
5 mM G-25-Hb <sup>c</sup>	13 $\pm$ 2	0.826 $\pm$ 0.127	15 $\pm$ 3	0.980 $\pm$ 0.196
5 mM 3xDEAE-Hb <sup>d</sup>	0.76 $\pm$ 0.1	0.048 $\pm$ 0.006	0.15 $\pm$ 0.1	0.01 $\pm$ 0.006
3xDEAE runoff <sup>e</sup>	17.2 $\pm$ 2.7	1.093 $\pm$ 0.172	18.3 $\pm$ 2.1	1.196 $\pm$ 0.137
5 mM dial-Hb <sup>f</sup>	1.7 $\pm$ 0.2	0.108 $\pm$ 0.01	1 $\pm$ 0.4	0.065 $\pm$ 0.026
250 mM GSNO	1.2 $\pm$ 0.8	0.076 $\pm$ 0.05	0.3 $\pm$ 0.1	0.019 $\pm$ 0.006
300 $\mu\text{M}$ CuZnSOD	612 $\pm$ 17	38.890 $\pm$ 1.080	578 $\pm$ 22	37.79 $\pm$ 1.438
15 mM DTPA	0.7 $\pm$ 0.3	0.044 $\pm$ 0.019	0.5 $\pm$ 0.2	0.032 $\pm$ 0.013
650 $\mu\text{M}$ neocuproine	1.6 $\pm$ 0.5	0.101 $\pm$ 0.031	0.9 $\pm$ 0.2	0.058 $\pm$ 0.013
200 mM NaPi buffer	0.9 $\pm$ 0.7	0.057 $\pm$ 0.044	1.1 $\pm$ 0.4	0.072 $\pm$ 0.026

<sup>a</sup> All stock solutions were prepared in 200 mM sodium phosphate buffer (pH 7.2). <sup>b</sup> Human Hb (Sigma) from the bottle; 5 mM Hb contains 20 mM heme. <sup>c</sup> Hb passed through a 1.6 cm  $\times$  2.5 cm G-25 column. <sup>d</sup> Hb passed 3 times through a 0.9 cm  $\times$  2.8 cm DEAE column. <sup>e</sup> Combined DEAE runoffs collected after each passage of Hb through the DEAE column. Metal ion concentrations were corrected for dilution; 0.50 mL of Hb solution was loaded on the column, and a total of 3.0 mL of runoff collected. <sup>f</sup> Hb following dialysis vs EDTA.

all CuZnSOD. The third DEAE eluate ( $\sim 3\text{ mL}$ ) was desalted on the HiTrap column to give the CuZnSOD-free sample referred to here as 3xDEAE-Hb.

**SOD-Activity Assay.** Lyophilized bovine CuZnSOD (10 mg) from the bottle was dissolved in 1 mL of NaPi to give a  $\sim 300\text{ }\mu\text{M}$  stock solution ( $\epsilon_{258\text{ nm}} = 10.3\text{ mM}^{-1}\text{ cm}^{-1}$ ).<sup>32</sup> Pyrogallol stock (40 mM) in 10 mM HCl (trace-metal grade) and 50 mM Tris (ultrapure) adjusted to pH 8.2 with 0.5 M cacodylic acid were freshly prepared.<sup>33</sup> Samples of 0.373  $\mu\text{M}$  metHb in Triscacodylate buffer (pH 8.2) were added to a 1-cm quartz cuvette at 25 °C, followed by 200  $\mu\text{M}$  pyrogallol, and the absorbance at 320 nm read every 15 s over 5 min to monitor rates of pyrogallol oxidation. At the wavelength chosen, the spectra of oxidized pyrogallol and metHb exhibit a maximum and minimum, respectively. Assuming 0% SOD activity in the blank [0.375  $\mu\text{M}$  3xDEAE-metHb] and 100% in the standard [0.375  $\mu\text{M}$  3xDEAE-metHb + 1.5 nM CuZnSOD monomer], we determined the relative SOD activities (and CuZnSOD concentrations) in the unknowns (X) from the initial slopes of the plots of 320-nm absorbance vs time:

$$\% \text{ relative SOD activity} = \left( \frac{3\text{xDEAE-metHb slope} - X \text{ slope}}{3\text{xDEAE-metHb slope} - \text{standard slope}} \right) \times 100 \quad (6)$$

**Western Blotting.** Western blotting was performed on a 5 mM Hb sample using the polyclonal antibody diluted to 1/500.<sup>34</sup> The blot was probed with the goat anti-rabbit-HRP secondary antibody, and the presence of CuZnSOD was detected by chemiluminescence following 1-s X-ray exposure.

**Spectrophotometric Titration of CuZnSOD with Neocuproine.** Solutions containing purified CuZnSOD were titrated with neocuproine to establish the time course of removal of active-site Cu<sup>I</sup> from the protein.<sup>35</sup> GSH was added to the CuZnSOD solutions  $\sim 30\text{ s}$  before neocuproine to convert Cu<sup>II</sup> to Cu<sup>I</sup>, and formation of the [Cu<sup>I</sup>(neocuproine)<sub>2</sub>]<sup>+</sup> complex was monitored spectrophotometrically ( $\epsilon_{454\text{ nm}} = 7950\text{ M}^{-1}\text{ cm}^{-1}$ ) following extraction with an equal volume of isoamyl alcohol.<sup>36</sup>

## Results

**ICP-MS Analysis.** The results summarized in Table 1 reveal that  $\sim 20\text{ }\mu\text{M}$  Cu and 20  $\mu\text{M}$  Zn are present in 5 mM solutions

(30) Antonini, E.; Brunori, M. *Hemoglobin and Myoglobin in Their Reactions with Ligands*; North-Holland Publishing Company: Amsterdam, 1971; Vol. 21.

(31) Williams, W. J.; Beantler, E.; Erslev, A. J.; Rundles, R. W. *Hematology*; McGraw-Hill Book Company A Blakisten Publication: New York, 1972; p 11.

(32) McCord, J. M.; Fridovich, I. *J. Biol. Chem.* **1969**, *244*, 6049–6055.

(33) Marklund, S.; Marklund, G. *Eur. J. Biochem.* **1974**, *47*, 469–474.

(34) Kurobe, N.; Suzuki, F.; Okajima, K.; Kato, K. *Clin. Chim. Acta* **1990**, *187*, 11–20.

(35) Liu, S. X.; Fabisiak, J. P.; Tyurin, V. A.; Borisenko, G. G.; Pitt, B. R.; Lazo, J. S.; Kagan, V. E. *Chem. Res. Toxicol.* **2000**, *13*, 922–931.

(36) Dohl, H.; Smith, G. F. *The Copper Reagents: Cuproine, Neocuproine, Bathocuproine*, 2nd ed.; The G. Frederick Smith Chemical Company: 1972.

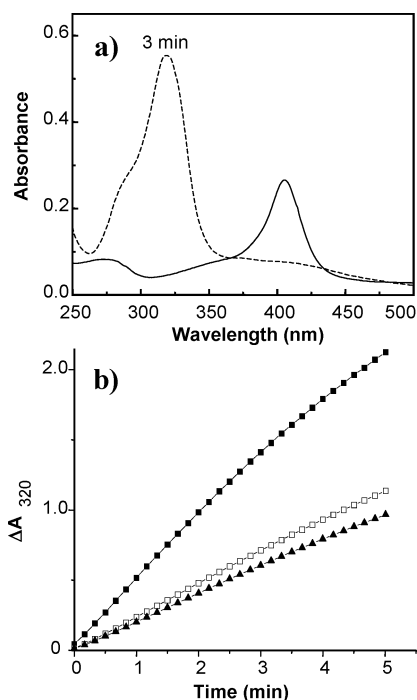
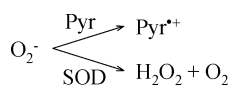


**Figure 1.** SOD-activity assay based on competition between CuZnSOD and pyrogallol for  $O_2^-$  in solutions containing metHb. (a) Spectrum of 0.375  $\mu\text{M}$  metHb (—) and of 200  $\mu\text{M}$  pyrogallol following autoxidation for 3 min (---). Spectra were recorded in a 1-cm quartz cuvette at 25  $^\circ\text{C}$  with a scan time of 1200 nm/min. (b) Time course of absorbance change at 320 nm following addition of 200  $\mu\text{L}$  pyrogallol to (■) 0.375  $\mu\text{M}$  3xDEAE-metHb; (□) 0.375  $\mu\text{M}$  3xDEAE-metHb + 1.5 nM CuZnSOD monomer; (▲) buffer only. Assays were carried out in 50 mM Triscacodylic acid buffer (pH 8.2) at 25  $^\circ\text{C}$  in a 3-mL quartz cuvette with a 1-cm path length.

of commercial human Hb. These concentrations are close to those found in RBCs, which contain  $\sim 5$  mM Hb<sup>31</sup> and  $\sim 20$   $\mu\text{M}$  CuZnSOD monomer.<sup>13</sup> Following dialysis or 3xDEAE purification, the Cu and Zn levels decreased to those ( $\sim 1$   $\mu\text{M}$ ) found in the buffer (Table 1). The metal ions were removed from CuZnSOD by EDTA chelation during dialysis,<sup>32</sup> whereas CuZnSOD ( $pI = 8.88$ )<sup>37</sup> was separated from Hb ( $pI = 7.15$ )<sup>30</sup> during anion-exchange chromatography because of their different affinities for the DEAE column. A CuZnSOD monomer concentration of  $\sim 15$   $\mu\text{M}$  per 5 mM Hb was determined by Western blotting (data not shown) in good agreement with the ICP-MS data (Table 1).

**SOD Activity Assay.** The spectra of oxidized pyrogallol and metHb exhibit a maximum and minimum, respectively, at 320 nm (Figure 1a). Relative rates of pyrogallol oxidation (Table 2) were determined from the initial linear portion of the plots of  $\Delta A_{320}$  vs time (Figure 1b). Clearly, 3xDEAE-metHb catalyzes pyrogallol oxidation (Figure 1b and Table 2) so the blank contained pyrogallol plus 3xDEAE-metHb. In solutions containing both pyrogallol and CuZnSOD, there is competition for the  $O_2^-$  produced:<sup>33</sup>



$\text{Pyr}^{*+}$  is the pyrogallol radical that dimerizes to form the colored product monitored at 320 nm,<sup>33</sup> and rates of pyrogallol oxidation

**Table 2.** Relative SOD Activities and CuZnSOD Concentrations of the metHb Samples

sample <sup>a</sup>	$\Delta A_{320}/\text{min}$	% relative activity <sup>c</sup>	CuZnSOD/5 mM Hb <sup>d</sup> ( $\mu\text{M}$ )
3xDEAE-Hb <sup>e</sup>	0.702	0	0
3xDEAE-Hb + 1.5 nM SOD	0.381	100 $\pm$ 2.0	20 $\pm$ 0.4
Dial-Hb <sup>e</sup>	0.656	14 $\pm$ 3.0	3 $\pm$ 0.6
G-25-Hb <sup>e</sup>	0.463	74 $\pm$ 5.0	15 $\pm$ 1.0
Hb <sup>e</sup>	0.358	107 $\pm$ 3.5	21 $\pm$ 0.7
buffer	0.324 <sup>f</sup>		

<sup>a</sup> Samples contained 0.375  $\mu\text{M}$  human metHb, and 1.5 nM bovine CuZnSOD monomer where indicated, in Triscacodylate buffer (pH 8.2) at 25  $^\circ\text{C}$ . The assay was initiated by adding 200  $\mu\text{M}$  pyrogallol. <sup>b</sup> Initial change in absorbance at 320 nm vs time due to pyrogallol oxidation. <sup>c</sup> Defined by eq 6 in the text. <sup>d</sup> Concentrations of active CuZnSOD monomer in the metHb solutions. Values are normalized to 5 mM Hb. <sup>e</sup> See footnotes b, c, d, and f, Table 1. <sup>f</sup> Rate of 200  $\mu\text{M}$  pyrogallol autoxidation in the Triscacodylate assay buffer (pH 8.2) at 25  $^\circ\text{C}$ .

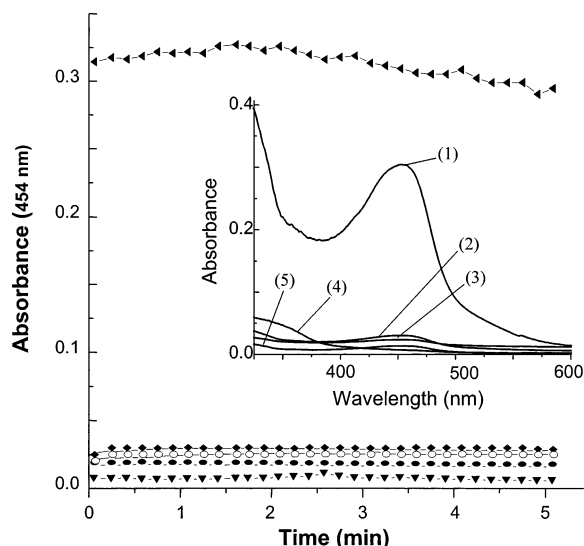
decrease in metHb samples when CuZnSOD is present (Figure 1b). The standard containing 0.375  $\mu\text{M}$  3xDEAE-metHb + 1.5 nM CuZnSOD monomer, which coincidentally exhibits the same initial rate of pyrogallol oxidation as observed in the buffer alone (Figure 1b), is arbitrarily assigned 100% CuZnSOD activity (Table 2), and the relative activities of the metHb samples are listed in Table 2. The  $\sim 107\%$  relative activity in 0.357  $\mu\text{M}$  untreated metHb corresponds to 1.5 nM CuZnSOD monomer or 20  $\mu\text{M}$  CuZnSOD monomer per 5 mM Hb, in excellent agreement with the ICP-MS data (Table 1). Dialysis versus EDTA is less effective than 3xDEAE purification in removing CuZnSOD activity since the Dial-Hb sample exhibits 14% relative SOD activity (Table 2). Re-uptake of trace copper and zinc by the apoSOD remaining after dialysis would give rise to the observed SOD activity. G-25-purified metHb (G-25-Hb) retains 74% of its SOD activity, which is not surprising given the fractionation range for globular proteins (1000–5000 Da) of this molecular-exclusion gel.<sup>38</sup>

Figure 2 shows that neocuproine reacts promptly with  $\text{CuSO}_4$  but not CuZnSOD in the presence of GSH to form  $[\text{Cu}^{\text{I}}(\text{neocuproine})_2]^+$ , which absorbs strongly at 454 nm (Figure 2, inset). Thus,  $\text{Cu}^{\text{I}}$  removal from CuZnSOD and chelation do not explain the loss of NO-transferase activity (reactions 3 and 4) in samples containing neocuproine. Addition of both neocuproine and DTPA does not increase the yield of  $[\text{Cu}^{\text{I}}(\text{neocuproine})_2]^+$  formation (Figure 2) suggesting that the combination of DTPA and neocuproine does not promote prompt copper removal from the enzyme. We have evidence that DTPA binds to CuZnSOD (Mengwei Ye, unpublished observations), which could also explain why DTPA inhibits the NO-transferase but not the SOD activity (reactions 1 and 2) of CuZnSOD (data not shown). DTPA-binding likely alters interaction of larger molecules such as GSNO or Hb with CuZnSOD but allows the small  $O_2^-$  substrate to access the active site. Further studies on chelator binding to CuZnSOD are underway.

**Visible Absorption Spectra of the Hb Incubates.** No reaction occurred at the heme during a 5-min incubation of 3.75 mM oxyHb (15 mM heme) with 7.5 mM GSNO (Cys $\beta$ 93/GSNO = 1) or 3.75 mM GSNO (Cys $\beta$ 93/GSNO = 2) (Figure 3). This indicates that all NO released from GSNO was directed

(37) Barra, D.; Martini, F.; Bannister, J. V.; Schinina, M. E.; Rotilio, G.; Bannister, W. H.; Bossa, F. *FEBS Lett.* **1980**, *120*, 53–56.

(38) Hagel, L. *Gel filtration. Protein Purification. Principles, high-resolution methods, and applications*; VCH Publishers Inc.: Weinheim, Cambridge, New York, 1989.



**Figure 2.** Formation of  $[\text{Cu}^{\text{I}}(\text{neocuproine})_2]^+$  in copper solutions.  $40 \mu\text{M}$  CuZnSOD monomer or  $40 \mu\text{M}$   $\text{CuSO}_4$  was added to  $200 \mu\text{M}$  GSH +  $80 \mu\text{M}$  neocuproine in  $200 \text{ mM}$  sodium phosphate buffer (pH 7.2), and following isoamyl alcohol extraction, the absorbance at  $454 \text{ nm}$  due to  $[\text{Cu}^{\text{I}}(\text{neocuproine})_2]^+$  was monitored vs time. The spectra after 5 min are shown in the insert. Sideway triangles and spectrum 1, neocuproine +  $\text{CuSO}_4$  + GSH. Diamonds ( $\blacklozenge$ ) and spectrum 2, CuZnSOD + neocuproine + GSH. Open circles ( $\circ$ ) and spectrum 3, CuZnSOD + neocuproine +  $20 \mu\text{M}$  DTPA + GSH. Solid circles ( $\bullet$ ) and spectrum 4, neocuproine + GSH. Inverted triangles ( $\blacktriangledown$ ) and spectrum 5, CuZnSOD + GSH.

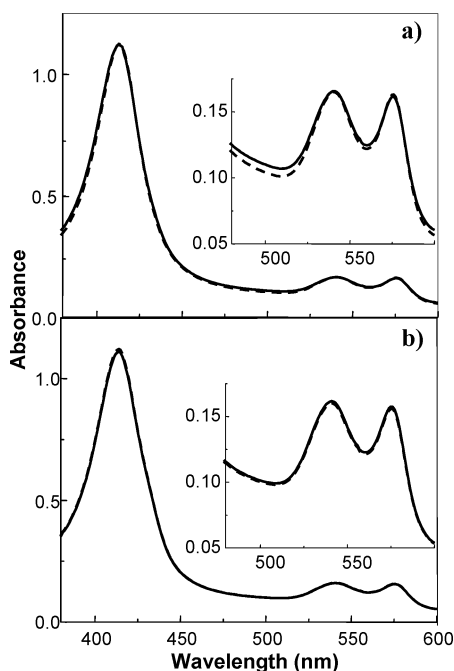


**Figure 3.** Effect of GSNO on the visible absorption spectrum of  $3.75 \text{ mM}$  oxyHb ( $15 \text{ mM}$  heme). (a) oxyHb (---); oxyHb +  $7.5 \text{ mM}$  GSNO (— $\times$ bd). (b) oxyHb (---); oxyHb +  $3.75 \text{ mM}$  GSNO (—). Spectra were recorded 5 min after mixing the reagents in  $200 \text{ mM}$  sodium phosphate buffer (pH 7.2) at  $25 \text{ }^\circ\text{C}$  in an FTIR-type cell with a  $6\text{-}\mu\text{m}$  Teflon spacer using a scan time of  $1200 \text{ nm/min}$ . This preparation of Hb was found to contain  $20 \mu\text{M}$  CuZnSOD monomer.

to Cys $\beta$ 93, which was confirmed by FTIR (Figure 6a) and ESI-MS (Figure 7b). The effect of CuZnSOD removal on the visible absorption spectra of  $3.75 \text{ mM}$  Hb ( $15 \text{ mM}$  heme) incubates was next examined. In a 5-min 3xDEAE-deoxyHb/GSNO incubate (Cys $\beta$ 93/GSNO = 1), no significant spectral changes were detected while  $\sim 100\%$  nitrosylHb (HbFe<sup>II</sup>NO) was formed

in the same incubate when bovine CuZnSOD was added (Figure 4a). However, when DTPA and neocuproine were also present, CuZnSOD addition had little effect on the spectrum of 3xDEAE-deoxyHb (data not shown), indicating that CuZnSOD-catalyzed GSNO breakdown is inhibited by the copper chelators. Interestingly, only 50% nitrosylHb was formed in the 5-min incubate when copper was added as  $\text{CuSO}_4$  (Figure 4a), although yields at longer times were not determined. Also, nitrosylHb formation was observed in the 5-min 3xDEAE-deoxyHb/DEA/NO incubate (Figure 4b), confirming that NO release from DEA/NO is not Cu-catalyzed.<sup>39,40</sup> The half-life of DEA/NO is  $\sim 8 \text{ min}$  at  $22 \text{ }^\circ\text{C}$  in  $100 \text{ mM}$  phosphate (pH 7.4), and it dissociates to give the free amine and 2 NO molecules following first-order kinetics.<sup>39</sup>

As expected, no reaction at the heme (Figure 4c) or Cys $\beta$ 93 (Figures 6b and 7a) was detected in 3xDEAE-oxyHb/GSNO incubates since GSNO breakdown, as monitored by nitrosylHb formation (Figure 4a), is prevented by CuZnSOD removal. Also, negligible spectral changes were observed in the 5-min 3xDEAE-oxyHb/GSNO incubate (Cys $\beta$ 93/GSNO = 1) in the presence of bovine CuZnSOD (Figure 4c), indicating that added bovine CuZnSOD, like human CuZnSOD (Figure 3), directs NO from GSNO to Cys $\beta$ 93 of oxyHb. Importantly, copper added as a Cu<sup>II</sup> salt does not direct all NO to Cys $\beta$ 93, since formation of metHb was detected in the 3xDEAE-oxyHb/GSNO/ $\text{CuSO}_4$  incubate (Cys $\beta$ 93/GSNO = 1; Figure 4c). Formation of metHb (via reaction 5) in the 5-min incubate of 3xDEAE-oxyHb/DEA/NO (Figure 4d) confirms that CuZnSOD is required to target all NO to Cys $\beta$ 93 of oxyHb.

From Figure 5, it can be deduced that NO targeting by CuZnSOD is insignificant in solutions containing  $0.5 \mu\text{M}$  Hb ( $2 \mu\text{M}$  heme) and  $1 \mu\text{M}$  GSNO (Cys $\beta$ 93/GSNO = 1). NitrosylHb and metHb formation can be clearly detected in the 5-min incubates of deoxyHb/GSNO (Figure 5a) and oxyHb/GSNO (Figure 5b), respectively, with and without chelators. This reveals that CuZnSOD does not target NO to Cys $\beta$ 93 at protein concentrations much lower than their physiological values. Also, the 100-fold lower concentration of chelators used in the experiments in Figure 5 versus Figure 4 does not inhibit redox turnover of CuZnSOD.

**FTIR Spectra of the Hb Incubates.** FTIR spectroscopy is a valuable probe of protein thiols since  $\nu(\text{SH})$  falls in a spectral window ( $\sim 2500 \text{ cm}^{-1}$ ) with minimum H<sub>2</sub>O and protein absorption.<sup>41,42</sup> Although  $> 1 \text{ mM}$  Hb is necessary to observe the weak IR  $\nu(\text{SH})$  absorption,<sup>41,42</sup> the concentrations used are comparable to those found in RBCs ( $\sim 5 \text{ mM}$  Hb).<sup>31</sup> The FTIR spectrum of  $7 \text{ mM}$  oxyHb recorded in the absence of GSNO (Figure 6) clearly exhibits the three  $\nu(\text{SH})$  peaks at 2586, 2566, and  $2553 \text{ cm}^{-1}$  assigned previously to Cys $\beta$ 93, Cys $\beta$ 112, and Cys $\alpha$ 104, respectively.<sup>41</sup>

A 5-min incubation of oxyHb with GSNO results in total loss of the Cys $\beta$ 93  $\nu(\text{SH})$  band when Cys $\beta$ 93/GSNO = 1 while 50% intensity remains in incubates with Cys $\beta$ 93/GSNO = 2 (Figure 6a). A 3xDEAE-oxyHb/GSNO incubate (Cys $\beta$ 93/GSNO = 1) did not show any loss of Cys $\beta$ 93  $\nu(\text{SH})$  intensity, but the

(39) Maragos, C. M.; Morley, D.; Wink, D. A.; Dunams, T. M.; Saavedra, J. E.; Hoffman, A.; Bove, A. A.; Isaac, L.; Hrabie, J. A.; Keefer, L. K. *J. Med. Chem.* **1991**, *34*, 3242–3247.

(40) Williams, D. L. H. *Chem. Commun.* **1996**, 1085–1091.

(41) Sampath, V.; Zhao, X. J.; Caughey, W. S. *Biochem. Biophys. Res. Commun.* **1994**, *198*, 281–287.

(42) Kandori, K. *J. Am. Chem. Soc.* **1998**, *120*, 5828–5829.

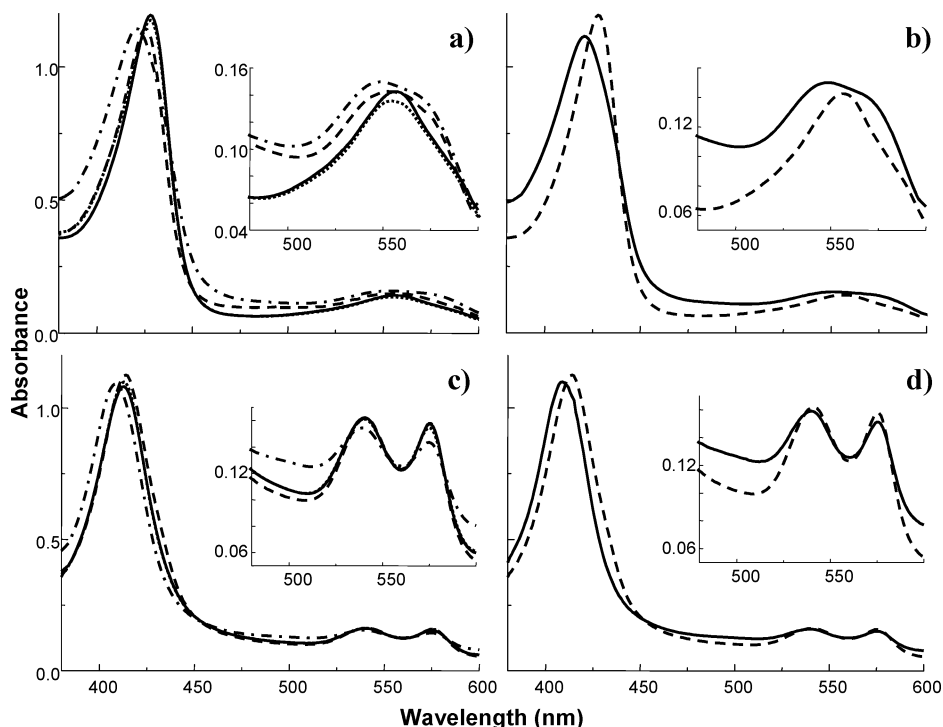
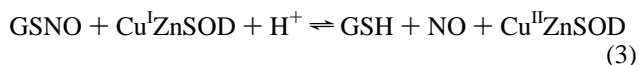


**Figure 4.** Effect of GSNO and 10  $\mu\text{M}$  CuZnSOD monomer or 10  $\mu\text{M}$   $\text{CuSO}_4$  on the visible absorption spectrum of 3.75 mM 3xDEAE-Hb (15 mM heme). (a) deoxyHb (—); deoxyHb + 7.5 mM GSNO ( $\cdots$ ); deoxyHb + 7.5 mM GSNO + CuZnSOD ( $-\cdot-$ ); deoxyHb + 7.5 mM GSNO +  $\text{CuSO}_4$  ( $---$ ). (b) deoxyHb ( $---$ ); deoxyHb + 3.75 mM DEA/NO (—). (c) oxyHb ( $---$ ); oxyHb + 7.5 mM GSNO + CuZnSOD + 200  $\mu\text{M}$  DTPA + 200  $\mu\text{M}$  neocuproine ( $\cdots$ ); oxyHb + 7.5 mM GSNO +  $\text{CuSO}_4$  ( $-\cdot-$ ); oxyHb + 7.5 mM GSNO + CuZnSOD (—). (d) oxyHb ( $---$ ); oxyHb + 3.75 mM DEA/NO (—). Spectra were recorded 5 min after mixing the reagents in 200 mM sodium phosphate buffer (pH 7.2) at 25  $^\circ\text{C}$  in a FTIR-type cell with a 6- $\mu\text{m}$  Teflon spacer using a scan time of 1200 nm/min. 3xDEAE-Hb contains no SOD activity.

band disappeared when 20  $\mu\text{M}$  monomer bovine CuZnSOD was added (Figure 6b). In contrast, <50% loss of Cys $\beta$ 93 absorbance was observed on addition of 20  $\mu\text{M}$   $\text{CuSO}_4$  (Figure 6b), confirming the partial oxyheme scavenging of NO released in the presence of free copper (Figure 4c). Addition of DTPA and neocuproine inhibited the NO-transferase activity of CuZnSOD (Figure 6b) consistent with the inhibition of CuZnSOD-catalyzed GSNO breakdown seen in Figure 4a.

**ESI-MS Results.** The deconvolved mass spectrum of Hb from the 5-min incubate of 7 mM 3xDEAE-oxyHb (28 mM heme) and 14 mM GSNO showed no evidence of  $\beta$ -subunit S-nitrosation (Figure 7a), while a peak with an increased mass of 29 Da is observed when bovine CuZnSOD was added to the incubate (Figure 7b). Interestingly, no Hb nitrosation is detected in the 5-min incubate of 0.5  $\mu\text{M}$  oxyHb (2  $\mu\text{M}$  heme) with 1  $\mu\text{M}$  GSNO (Figure 7c).

An intense peak due to GSSGH $^+$  ( $m/z$  613.5) is observed in the ESI mass spectrum of a 5-min GSH/GSNO/CuZnSOD incubate (Figure 8a, insert). Presumably, GSSG is formed in the CuZnSOD-catalyzed reductive cleavage of GSNO:

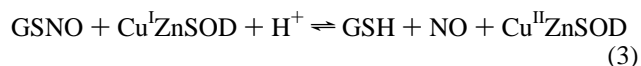
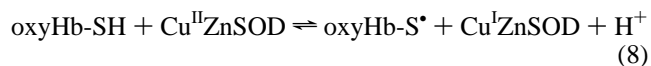


In contrast, no GSSGH $^+$  peak appears in the spectrum of the 5-min 3xDEAE-oxyHb/GSNO/CuZnSOD incubate (Figure 8b, insert) indicating that the GSH formed in situ (eqn 3) does not supply electrons for GSNO reductive cleavage in this incubate. GSSG formation in the 3xDEAE-oxyHb/GSNO/ $\text{CuSO}_4$  (data not shown) and deoxyHb/GSNO incubates, $^{11}$  and in all incubates

containing 0.5  $\mu\text{M}$  Hb (data not shown), signals that GSH is oxidized. Combined, these results reveal that GSH acts an electron donor in all the Hb/GSNO incubates examined except in those containing oxyHb(mM)/GSNO/CuZnSOD where all of the released NO is directed to Cys $\beta$ 93.

## Discussion

We have previously shown that copper redox turnover is required for oxyHb S-nitrosation by GSNO $^1$ . In the present work, we demonstrate that commercial human Hb contains  $\sim$ 20  $\mu\text{M}$  CuZnSOD monomer and that the latter is a highly efficient catalyst of NO transfer from millimolar GSNO to Cys $\beta$ 93 of oxyHb at the concentrations of Hb ( $\sim$ 5 mM) $^{31}$  and CuZnSOD (20  $\mu\text{M}$  monomer) $^{13}$  found in RBCs. The well-documented $^{17,43}$  reaction of NO with oxyHb (eq 5) dominates at micromolar Hb (Figure 5) but not at physiological concentrations of oxyHb and CuZnSOD, where all the NO released is directed to Cys $\beta$ 93 (Figures 3 and 6). The following mechanism for CuZnSOD-catalyzed NO transfer from GSNO to Cys $\beta$ 93 is proposed:



Formation of a thiyl radical on Cys $\beta$ 93 should produce an efficient scavenger of the NO released on reductive cleavage of GSNO. Since glutathiolation of Cys $\beta$ 93 (Hb-SSG forma-

(43) Artz, J. D.; Thatcher, G. R. J. *Chem. Res. Toxicol.* **1998**, *11*, 1394–1397.

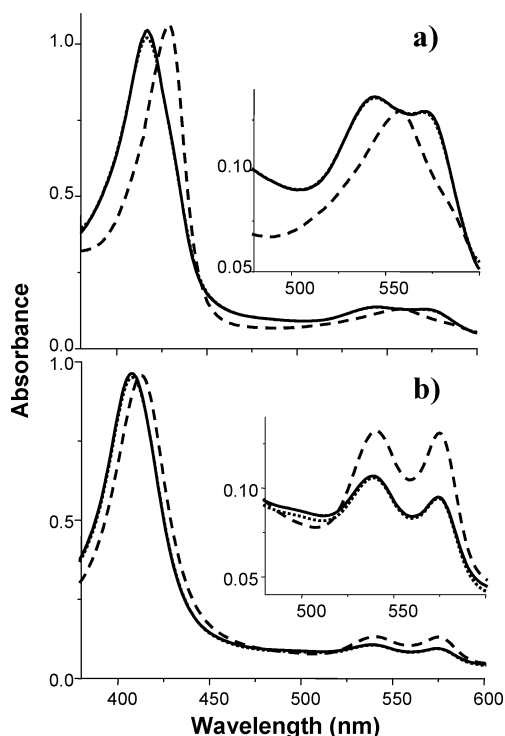


**Figure 5.** Effect of 1  $\mu\text{M}$  GSNO on the visible absorption spectrum of 0.5  $\mu\text{M}$  Hb (2  $\mu\text{M}$  heme). (a) deoxyHb (---); deoxyHb + GSNO (—); deoxyHb + GSNO + 2  $\mu\text{M}$  DTPA + 2  $\mu\text{M}$  neocuproine (···). (b) oxyHb (---); oxyHb + GSNO (—); oxyHb GSNO + 2  $\mu\text{M}$  DTPA + 2  $\mu\text{M}$  neocuproine (···). Spectra were recorded 5 min after mixing the reagents in 200 mM sodium phosphate buffer (pH 7.2) at 25  $^{\circ}\text{C}$  in a 1-cm quartz cuvette using a scan time of 1200 nm/min.

tion)<sup>44</sup> was not detected by mass spectrometry, the putative thiyl radical would have to be more reactive with NO than with the GSH generated in reaction 3.

It is further proposed that, at  $\sim 5$  mM oxyHb, reactions 8, 3, and 9 all occur within an oxyHb–CuZnSOD encounter complex. The proteins are presumably oriented with respect to each other within this complex to target or channel the nascent NO to the thiyl radical on Cys $\beta$ 93 and thereby prevent its scavenging by the Fe<sup>II</sup>O<sub>2</sub> heme (reaction 5). Our key finding is that *all* the NO released from GSNO is targeted to Cys $\beta$ 93 at physiological concentrations of oxyHb and CuZnSOD (Figures 3 and 6). When CuZnSOD is removed, and GSNO breakdown is catalyzed by added CuSO<sub>4</sub>, the released NO is scavenged by both Cys $\beta$ 93 (Figure 6b) and the Fe<sup>II</sup>O<sub>2</sub> heme (Figure 4C). Thus, in the presence of CuZnSOD, the transient oxyHb–S\* would have to be formed close to the site of NO generation to prevent scavenging by the Fe<sup>II</sup>O<sub>2</sub> heme. Such efficient channeling of NO would require the formation of an oriented encounter complex between oxyHb and CuZnSOD. Furthermore, since product analysis revealed that no GSSG was formed in the 3xDEAE-oxyHb/GSNO/CuZnSOD incubate (Figure 8b), the GSH generated in situ (reaction 3) is not kinetically competitive with Cys $\beta$ 93 as an electron donor to Cu<sup>II</sup>ZnSOD. The dominance of reaction 8 over reaction 7 provides additional evidence for the formation of an encounter complex between the proteins, since positioning Cys $\beta$ 93 close to the active site of CuZnSOD in an oxyHb–CuZnSOD complex would ensure that the protein-

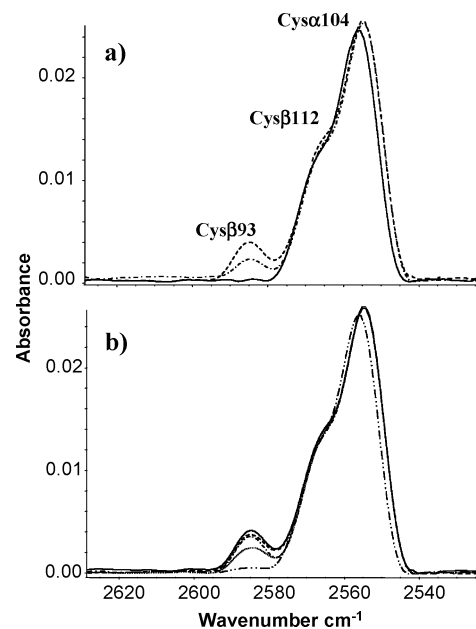


**Figure 6.** Effect of GSNO on the FTIR spectrum in the  $\nu(\text{SH})$  region of 7.0 mM oxyHb (28 mM heme). (a) oxyHb (---); oxyHb + 7 mM GSNO (- · -); oxyHb + 14 mM GSNO (—). (b) 3xDEAE-oxyHb (—); 3xDEAE-oxyHb + 14 mM GSNO (---); 3xDEAE-oxyHb + 14 mM GSNO + 20  $\mu\text{M}$  CuZnSOD monomer + 500  $\mu\text{M}$  DTPA + 200  $\mu\text{M}$  neocuproine (- · -); 3xDEAE-oxyHb + 14 mM GSNO + 20  $\mu\text{M}$  CuSO<sub>4</sub> (···); 3xDEAE-oxyHb + 14 mM GSNO + 20  $\mu\text{M}$  CuZnSOD monomer (- · -). Spectra were recorded in a 250- $\mu\text{m}$  path length FTIR cell 5 min after mixing the reagents in 200 mM sodium phosphate buffer (pH 7.2) at 25  $^{\circ}\text{C}$  and are the average of 500 scans at 2-cm<sup>-1</sup> resolution. Background subtraction, baseline correction, smoothing, and Fourier transform self-deconvolution were performed on the displayed spectra (see text).

bound thiol acts as an electron donor to the Cu<sup>II</sup>. Complex formation could also allow Cys $\beta$ 93 ( $\sim 10$  mM)<sup>31</sup> to compete with GSH ( $\sim 5$  mM)<sup>45</sup> as an electron donor to Cu<sup>II</sup>ZnSOD under physiological conditions, although the kinetics are yet to be determined. On dilution of the reagents, most of the NO released from GSNO is scavenged by the Fe<sup>II</sup>O<sub>2</sub> heme (Figure 5b), no Cys $\beta$ 93 S-nitrosation is detected (Figure 7c), and GSSG is formed (data not shown) revealing that GSH is an electron donor. These observations suggest the absence of an oxyHb/CuZnSOD encounter complex at low Hb concentrations and the loss of NO channeling to Cys $\beta$ 93.

The levels of GSNO used here are up to 10<sup>6</sup>-fold higher than those expected in vivo, which are generally reported to be in the nanomolar range.<sup>8,18,20–22</sup> The mechanism of NO transfer from nanomolar GSNO to millimolar Hb cannot be probed *directly* using visible and infrared absorption measurements as done here. However, if 20  $\mu\text{M}$  CuZnSOD monomer catalyzes the channeling of *all* NO from 3.25 or 7.5 mM GSNO to 7.5 mM Cys $\beta$ 93 of oxyHb (Figures 3 and 6), we assume that it catalyzes the channeling of *all* NO from nanomolar GSNO to 10 mM Cys $\beta$ 93 in RBCs. The critical factor for NO channeling suggested by the results reported here is the presence of oxyHb–CuZnSOD encounter complexes, which are expected to be present in similar concentrations in RBCs and in cell-free solutions containing 5mM Hb and 20  $\mu\text{M}$  CuZnSOD monomer.

Control of NO capture at Cys $\beta$ 93 by the allosteric transition of Hb can also be rationalized based on reaction 8. In T-state Hb, which occurs on release of O<sub>2</sub>, Cys $\beta$ 93 must be a poor

(44) Rossi, R.; Barra, D.; Bellelli, A.; Boumis, G.; Canofeni, S.; Di Simplicio, P.; Lusini, L.; Pascarella, S.; Amiconi, G. *J. Biol. Chem.* **1998**, *273*, 19198–19206.

(45) Griffith, O. W. *Free Radical Biol. Med.* **1999**, *27*, 922–935.



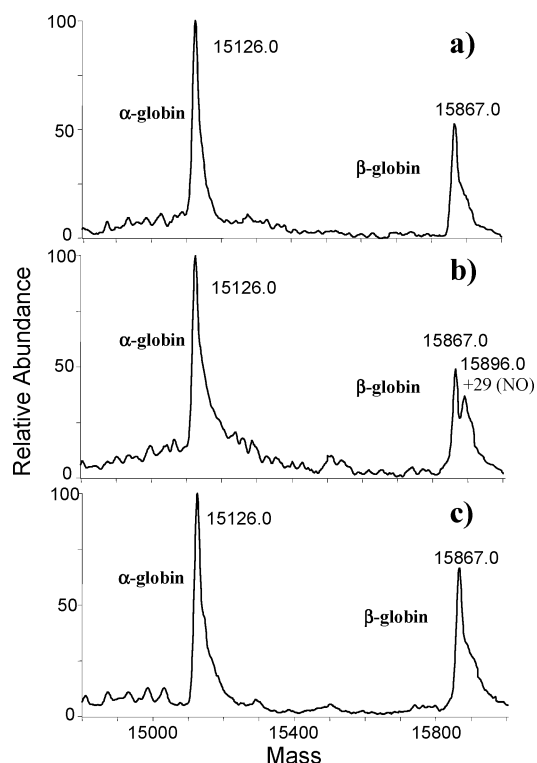
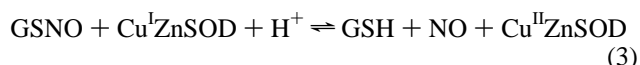


**Figure 7.** Effect of GSNO on the deconvoluted electrospray mass spectra of the heme-free Hb subunits. (a) Hb from 7.0 mM 3xDEAE-oxyHb + 14 mM GSNO incubate; (b) Hb from 7.0 mM 3xDEAE-oxyHb + 14 mM GSNO + 20  $\mu$ M CuZnSOD monomer incubate; (c) Hb from 0.5  $\mu$ M Hb + 1  $\mu$ M GSNO incubate. Experimental conditions: following incubation of the reactants in 200 mM sodium phosphate buffer (pH 7.2) for 5 min at 25  $^{\circ}$ C, the Hb concentration in spectra a and b was adjusted to 7  $\mu$ M ( $\sim$ 0.45  $\mu$ g/ $\mu$ L) by dilution in H<sub>2</sub>O. Aliquots (100  $\mu$ L) were infused into the ESI source of the mass spectrometer by flow injection at 50  $\mu$ L/min with 75% CH<sub>3</sub>CN/0.05% TFA as a mobile phase. The capillary temperature was 180  $^{\circ}$ C, and the spray voltage, 4.0 kV. Hb dissociated into free heme and  $\alpha$ - and  $\beta$ -subunits under the MS conditions. The unresolved shoulders on the subunit peaks at high mass are due to sodium adducts.

electron donor to Cu<sup>II</sup>ZnSOD since high concentrations of GSSG were detected in the ESI mass spectrum of deoxyHb/GSNO incubates.<sup>11</sup> This reveals that GSH formed in situ is the electron donor to Cu<sup>II</sup>ZnSOD, and in the absence of thiol radical formation on Cys $\beta$ 93, the NO released (reaction 3) is captured by the deoxyheme (Figure 4a) consistent with reports that Cys $\beta$ 93 of deoxyHb is not S-nitrosated.<sup>11,46</sup> In summary, the proposed reactions occurring in deoxyHb/GSNO incubates are the following:



Since Cu<sup>II</sup>-catalyzed RSNO formation is not kinetically competitive with disulfide formation for low-molecular-weight thiols,<sup>1,47</sup> the GS<sup>\*</sup> radicals, formed as intermediates in reaction 7, dimerize faster than they react with NO. This permits the nascent NO to be scavenged by the deoxyheme (reaction 10) in deoxyHb/GSNO incubates as seen in Figure 4a.

(46) Spencer, N. Y.; Zeng, H.; Patel, R. P.; Hogg, N. *J. Biol. Chem.* **2000**, *275*, 36562–36567.

(47) Noble, D. R.; Williams, D. L. *Nitric Oxide* **2000**, *4*, 392–398.

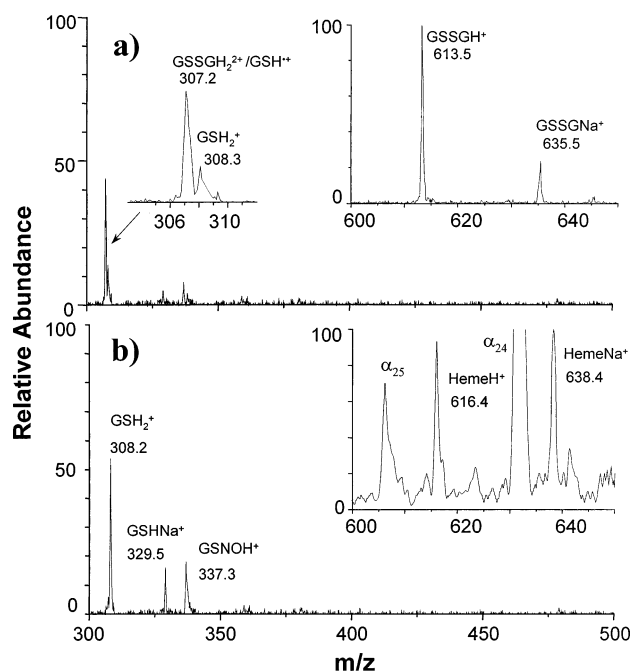


**Figure 8.** Electrospray mass spectral analysis of the glutathione-derived products. (a) 14 mM GSNO + 14 mM GSH + 20  $\mu$ M CuZnSOD monomer; (b) 7.0 mM 3xDEAE-oxyHb + 14 mM GSNO + 20  $\mu$ M CuZnSOD monomer. Experimental conditions: following incubation of the reactants in 200 mM sodium phosphate buffer (pH 7.2) for 5 min at 25  $^{\circ}$ C, the samples were diluted 10<sup>3</sup>-fold and the mass spectra recorded as outlined in Figure 7. Peaks labeled  $\alpha_{24}$  and  $\alpha_{25}$  are due to  $\alpha$ -globinH<sub>24</sub><sup>24+</sup> and  $\alpha$ -globinH<sub>25</sub><sup>25+</sup>, respectively. Peak intensities in spectrum a are relative to the GSSGH<sup>+</sup> peak at  $m/z$  613.5 (100%) and, in spectrum b, to the hemeNa<sup>+</sup> peak at  $m/z$  638 (100%). GSH<sup>+</sup> formed on the homolysis and protonation in the ESI source of residual GSNO could also contribute to the intensity of the peak at  $m/z$  307 in spectrum a.

Copper added as CuSO<sub>4</sub> is less efficient than CuZnSOD in catalyzing the reductive cleavage of GSNO, giving rise to only  $\sim$ 50% yield of nitrosylHb within 5 min (Figure 4a). This could be explained by the binding of free Cu<sup>II</sup> to Hb, which possesses two well-characterized copper binding sites,<sup>48</sup> and/or complexation of Cu<sup>II</sup> by GSSG.<sup>47</sup> However, CuSO<sub>4</sub> not only is a less efficient catalyst of GSNO reductive cleavage but also does not target *all* the NO released from GSNO to Cys $\beta$ 93 in oxyHb incubates (Figures 4b and 6b). As mentioned previously, this observation supports channeling of NO from GSNO to Cys $\beta$ 93 within an oxyHb–CuZnSOD encounter complex. Also, the NO spontaneously released from DEA/NO<sup>39</sup> is directed to the Fe<sup>II</sup>O<sub>2</sub> heme (Figure 4d), presumably because no protein thiol radicals are formed in oxyHb incubates with DEA/NO to scavenge the NO (reaction 9).

To fully assess on a chemical basis the highly controversial hypothesis that Hb delivers NO to tissues in a pO<sub>2</sub>-dependent manner,<sup>2</sup> elucidation of the conditions that promote NO release from Cys $\beta$ 93, as well as from nitrosylHb, is necessary. Hb denitrosation could conceivably also involve redox turnover of CuZnSOD. Using electrons donated from GSH (reaction 7), Cu<sup>I</sup>-ZnSOD could catalyze Cys $\beta$ 93-SNO breakdown to give the free thiol and NO. This would be reversible for oxyHb, which undergoes reactions 8 and 9 but not for deoxyHb, consistent with the proposal that O<sub>2</sub> release from Hb promotes NO release from Cys $\beta$ 93.<sup>7</sup> We are currently investigating the stability of

(48) Antholine, W. E.; Taketa, F.; Wang, J. T.; Manoharan, P. T.; Rifkind, J. M. *J. Inorg. Biochem.* **1985**, *25*, 95–108.

performed Hb-SNO in the presence of CuZnSOD and different concentrations of GSH. Given the complexity of these reactions, to understand the possible mechanisms of Hb-SNO formation and breakdown *in vivo*, it is necessary to separate the S-nitrosation and denitrosation steps.

### Conclusions

Erythrocyte CuZnSOD may play a role in vasorelaxation by targeting NO to Cys $\beta$ 93 of oxyHb and thereby preventing NO scavenging by the Fe<sup>II</sup>O<sub>2</sub> heme at physiological concentrations of the proteins. The allosteric transition of Hb controls the products formed in CuZnSOD-catalyzed NO transfer from GSNO to Hb since NO is channeled to Cys $\beta$ 93 in oxyHb incubates but scavenged by the heme in deoxyHb incubates. Although millimolar GSNO was used to *directly* probe the products formed, the results may also be relevant at physiological (nanomolar) GSNO concentrations since a critical factor appears to be the formation of an oxyHb–CuZnSOD encounter complex to ensure NO channeling. Conversion of NO to NO<sub>3</sub><sup>-</sup>, which is nonvasoactive, occurs in the absence of CuZnSOD or at oxyHb concentrations  $\sim 10^3$ -fold below physiological values, conditions that may eliminate or disrupt oxyHb–CuZnSOD complexation.

The results presented here may also hold far-reaching implications in cell signaling. Like protein phosphorylation,

protein S-nitrosation may represent a fundamental mechanism for the reversible post-translational control of protein activity and cellular function.<sup>49</sup> The reaction scheme defined by eqs 8, 3, and 9 suggests a general mechanism for selectivity in protein S-nitrosation. Only proteins with cysteine residues that can act as donors to an NO-transferase such as CuZnSOD will be S-nitrosated. Colocalization of the donor and transferase, as occurs in RBCs for oxyHb and CuZnSOD, will promote S-nitrosation of the target, which in the present *in vitro* study serves to prevent the conversion of NO to NO<sub>3</sub><sup>-</sup>.

**Acknowledgment.** This research was supported by grants from CIHR, NSERC (Canada), FQRNT (Quebec) to A.M.E. and J.A.C. and by a Graduate Fellowship (Concordia University) to A.A.R. We would like to thank Professor Eric Salin and Margaret Antler from the Department of Chemistry, McGill University, for helping us with the ICP-MS measurements and for the use of their ICP-MS instrumentation. Drs. Jeff Agar and Heather Durham from the Montreal Neurological Institute are thanked for their help in the Western blotting experiments.

JA0289752

(49) Hoffmann, J.; Haendeler, J.; Zeiher, A. M.; Dimmeler, S. *J. Biol. Chem.* **2001**, *276*, 41383–41387.